# Deterministic Attitude Estimation

Abraham P. Vinod* and Arun D. Mahindrakar†

July 2, 2016

## 1 Introduction

The rotation matrix is an effective tool to analyze the transformation between two coordinate frames independent of the relative motion of these frames. This linear transformation has been rigorously studied and plays an important part in the study of mechanical systems [1]. In the past few decades, the problem of attitude estimation of rigid bodies has been explored quite deeply in the context of attitude control[2][3]. Recently, with the study on UAVs [4], the requirement for practical and reliable implementations of attitude estimation have gained importance.

In this chapter, we provide an introduction to attitude estimation, emphasising on the implementation. We study two approaches for attitude estimation — deterministic and optimal. We attempt to elucidate the properties of the deterministic attitude estimation and discuss two deterministic attitude estimation algorithms — TRIAD [5] and DAESR [6]. For closure, an optimal attitude estimation is also studied. These algorithms are then discussed in a real-world setting using a spherical robot as a test-bench.

## 2 Preliminaries

We follow the definitions given in [1]. We use the convention of distinguishing between scalars and vectors/matrices using boldfaced text and distinguishing vectors from matrices using the lower letter case.

Let $\|\cdot\|$ denote the 2-norm on $\mathbb{R}^n$. The unit sphere in $\mathbb{R}^n$ is defined as $S^{n-1} = \{\boldsymbol{v} \in \mathbb{R}^n : \|\boldsymbol{v}\| = 1\}$. Specifically, $S^1 = (-\pi, \pi]$ denotes the set of angle naturally associated with a unit circle on a plane and $S^2$ is the set of unit vectors in $\mathbb{R}^3$. Let $\boldsymbol{I}_3$ denote the $3\times3$ identity matrix and the time-dependent orientation of a rigid body relative to the reference inertial frame be denoted by $\boldsymbol{R} \in SO(3)$ , where $SO(3) \triangleq \{\boldsymbol{A} \in \mathbb{R}^{3\times3} : \boldsymbol{A}^\top\boldsymbol{A} = \boldsymbol{I}_3, \det(\boldsymbol{A}) = 1\}$ and $\dot{\boldsymbol{R}} \in T_{\boldsymbol{R}}SO(3)$, the tangent space to $SO(3)$ at $\boldsymbol{R}$. Since $SO(3)$ is a Lie group, $T_{\boldsymbol{I}}SO(3) \simeq \mathfrak{so}(3)$ acts as Lie algebra of the group, where $\boldsymbol{I}_3$ is the identity element of the group $SO(3)$ and $\mathfrak{so}(3)$ is a vector space formed by $3 \times 3$ skew-symmetric matrices. Also, $\mathfrak{so}(3)$ is isomorphic to $\mathbb{R}^3$ which allows the definition of the wedge operator '$\wedge$'

*Abraham P. Vinod is with Electrical and Computer Engineering, University of New Mexico, Albuquerque, NM 87131 USA; e-mail: aby.vinod@gmail.com

†Arun D. Mahindrakar is with the Department of Electrical Engineering, Indian Institute of Technology Madras, Chennai-600036, India; email: arun_dm@iitm.ac.in

as $\boldsymbol{\nu} = \{x_1, x_2, x_3\} \in \mathbb{R}^3 \mapsto \widehat{\boldsymbol{\nu}} \in \mathfrak{so}(3)$:

$$\widehat{\boldsymbol{\nu}} = \begin{bmatrix} 0 & -x_3 & x_2 \\ x_3 & 0 & -x_1 \\ -x_2 & x_1 & 0 \end{bmatrix}.$$

The vee operator '$\vee$' is defined as the inverse of the wedge operation, that is, $(\widehat{\boldsymbol{\nu}})^{\vee} = \boldsymbol{\nu}$. For notational brevity, we have dropped the reference to the time-dependence of the rotation matrices.

From the formal definitions given above, we can represent $\boldsymbol{R}$ as an orthogonal matrix with unit determinant, that is, $\boldsymbol{R} \triangleq \begin{bmatrix} \boldsymbol{c}_1 & \boldsymbol{c}_2 & \boldsymbol{c}_3 \end{bmatrix} \triangleq \begin{bmatrix} \boldsymbol{r}_1 & \boldsymbol{r}_2 & \boldsymbol{r}_3 \end{bmatrix}^{\top}$ where the columns $(\boldsymbol{c}_1, \boldsymbol{c}_2, \boldsymbol{c}_3)$ and the rows $(\boldsymbol{r}_1, \boldsymbol{r}_2, \boldsymbol{r}_3)$ are mutually orthogonal vectors in $S^2$. The body angular velocity matrix, $\widehat{\boldsymbol{\omega}} \in \mathfrak{so}(3)$, associated with $\boldsymbol{R}$ is given by the relation $\widehat{\boldsymbol{\omega}} = (\boldsymbol{R}^{\top}\dot{\boldsymbol{R}})$. Using the $\vee$ operator, we define the angular velocity vector $\boldsymbol{\omega} = (\boldsymbol{R}^{\top}\dot{\boldsymbol{R}})^{\vee} \in \mathbb{R}^3$. Similarly, we define the spatial angular velocity matrix, $\widehat{\boldsymbol{\Omega}} \in \mathfrak{so}(3)$, as $\widehat{\boldsymbol{\Omega}} = (\dot{\boldsymbol{R}}\boldsymbol{R}^{\top})$ and the spatial angular velocity vector as $\boldsymbol{\Omega} = (\dot{\boldsymbol{R}}\boldsymbol{R}^{\top})^{\vee} \in \mathbb{R}^3$.

We denote an orthogonal coordinate frame using $\{\mathbb{F}\}$ and $\boldsymbol{R}_{F_2}^{F_1}$ maps vectors in $\{\mathbb{F}_2\}$ to $\{\mathbb{F}_1\}$. Composition of elements in $SO(3)$, the rotation matrices, happens through matrix multiplication. That is, the rotation matrix that maps vectors from $\{\mathbb{F}_3\}$ to $\{\mathbb{F}_1\}$ is given by $\boldsymbol{R}_{F_3}^{F_1} = \boldsymbol{R}_{F_2}^{F_1}\boldsymbol{R}_{F_3}^{F_2}$. By definition, $\boldsymbol{R}_{F_2}^{F_1} = (\boldsymbol{R}_{F_1}^{F_2})^{\top}$ since $\boldsymbol{R}_{F_2}^{F_1}\boldsymbol{R}_{F_1}^{F_2} = \boldsymbol{I}_3$.

## 2.1 Representations for attitude: Equivalent axis and Euler angle representation

This subsection provides a brief introduction to two popular representations for attitude — Equivalent axis and Euler angle representation. For a detailed discussion, the reader is directed to [1]

***Equivalent axis representation***: Euler's theorem is an important theorem in kinematics which defines a representation of attitude known as equivalent axis representation.

**Theorem 2.1 (Euler's theorem)** *Any orientation $\boldsymbol{R} \in SO(3)$ is equivalent to a rotation about a fixed axis $\boldsymbol{\eta} \in \mathbb{R}^3$ through an angle $\theta \in (-\pi, \pi]$.*

Equivalent axis representation is not unique for a given $\boldsymbol{R}$ since the exponential map is not injective. Also, this representation has two singularity points (conditions for indeterminateness) at $\theta = \{0, \pi\}$ because a $n$-dimensional closed manifold can not be embedded in $\mathbb{R}^n$ without having singularities.

Rodrigues' rotation formula allows us to obtain the rotation matrix corresponding to a unit vector and a rotation angle. The rotation matrix corresponding to a screw-angle pair $(\boldsymbol{\eta}, \theta)$ with $\boldsymbol{\eta} \in S^2,\ \theta \in S^1$ is given by

$$\boldsymbol{R}_{(\boldsymbol{\eta},\theta)} = \boldsymbol{I}_3 + \widehat{\boldsymbol{\eta}}\sin\theta + (\widehat{\boldsymbol{\eta}})^2(1 - \cos\theta). \tag{1}$$

As expected, the screw is invariant to the rotation transformation, or in other words, $\boldsymbol{\eta} = \boldsymbol{R}_{(\boldsymbol{\eta},\theta)}\boldsymbol{\eta}$. By convention, a positive $\theta$ implies an anti-clockwise rotation about $\boldsymbol{\eta}$. Rodrigues' rotation formula is used extensively in applications involving mechanics and image signal processing. This formula can also be used to find the linear transformation that links two vectors $\boldsymbol{v}, \boldsymbol{w} \in S^2$ $(\boldsymbol{v} \neq \pm\boldsymbol{w})$ by the relation $\boldsymbol{v} = \boldsymbol{R}_{\boldsymbol{w}\to\boldsymbol{v}}\boldsymbol{w}$ [7]. The

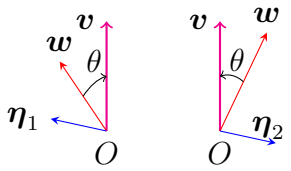


Figure 1: Figure defining screw-angle pair for the modified Rodrigues' formula

estimation of $\boldsymbol{R}_{\boldsymbol{w}\to\boldsymbol{v}}$ using (1) uses the following definitions:

$$\begin{aligned} \boldsymbol{\eta} &= \frac{\boldsymbol{w}\times\boldsymbol{v}}{\|\boldsymbol{w}\times\boldsymbol{v}\|} \text{ for } \boldsymbol{v}\neq\pm\boldsymbol{w} \\ \sin\theta &= \|\boldsymbol{w}\times\boldsymbol{v}\| \\ \cos\theta &= \boldsymbol{v}.\boldsymbol{w} \\ \theta &= atan2(\|\boldsymbol{w}\times\boldsymbol{v}\|, \boldsymbol{v}.\boldsymbol{w}) \in [0,\pi] \subset S^1. \end{aligned} \tag{2}$$

Note that $\theta \in [0,\pi]$, a subset of $S^1$. Equation (2) provides an equivalent axis representation of $\boldsymbol{R}_{\boldsymbol{w}\to\boldsymbol{v}}$ because of the definition of $\boldsymbol{\eta}$. As seen in Figure 1, depending on the position of $\boldsymbol{w}$ and $\boldsymbol{v}$, the rotation is always anti-clockwise with respect to their respective screws $\boldsymbol{\eta}_1$ and $\boldsymbol{\eta}_2$. Hence, for the representation where $\theta$ is negative (clockwise rotation), the definition of the screw is such that the rotation is anti-clockwise. Therefore, $(\boldsymbol{\eta},\theta) \in S^2\times[0,\pi]$ spans $SO(3)$.

The singularity in the equivalent axis representation occurs when $\boldsymbol{w} = \pm\boldsymbol{v}$ since no unique $\boldsymbol{\eta}$ exists. Also, as $\boldsymbol{w}$ approaches $\pm\boldsymbol{v}$, the determination of a unit vector $\boldsymbol{\eta}$ becomes increasingly erroneous owing to the division by a very small positive decimal number, $\sin\theta$.

The following modification to the equivalent axis representation given by (1) and (2) was proposed in [6] [8] to mitigate these disadvantages:

**Proposition 2.1** *Rodrigues' formula relating two vectors $\boldsymbol{w},\boldsymbol{v} \in S^2$ and $\boldsymbol{w} \neq -\boldsymbol{v}$ provided by* (1) *and* (2) *can be equivalently written as*

$$\boldsymbol{R}_{\boldsymbol{w}\to\boldsymbol{v}} = \boldsymbol{I}_3 + \widehat{\boldsymbol{\eta}^*} + \frac{\left(\widehat{\boldsymbol{\eta}^*}\right)^2}{1+\cos\theta} \tag{3}$$

*where*

$$\begin{aligned} \boldsymbol{\eta}^* &= \boldsymbol{w}\times\boldsymbol{v} \\ \cos\theta &= \boldsymbol{w}.\boldsymbol{v}. \end{aligned}$$

*Proof:* For $\boldsymbol{w},\boldsymbol{v} \in S^2$ and $\boldsymbol{\eta}^* = \boldsymbol{w}\times\boldsymbol{v}$, we know that $\sin\theta = \|\boldsymbol{w}\times\boldsymbol{v}\| = \|\boldsymbol{\eta}^*\|$ since $\theta \in [0,\pi]$. We can replace $\boldsymbol{\eta}$ in (1) with $\frac{\boldsymbol{\eta}^*}{\sin\theta}$ to account for the observation that $\boldsymbol{\eta}$ is not only the unit vector parallel to $\boldsymbol{\eta}^*$ but also switches its direction depending on the sign of $\theta$ (Figure 1). Replacing $\boldsymbol{\eta}$ in (1), we obtain

$$\boldsymbol{R}_{\boldsymbol{w}\to\boldsymbol{v}} = \boldsymbol{I}_3 + \widehat{\boldsymbol{\eta}^*} + \left(\widehat{\boldsymbol{\eta}^*}\right)^2 \frac{(1-\cos\theta)}{\sin^2\theta}. \tag{4}$$

The modified Rodrigues' formula thus is:

$$\begin{aligned} \boldsymbol{R}_{\boldsymbol{w}\to\boldsymbol{v}} &= \boldsymbol{I}_3 + \widehat{\boldsymbol{\eta}^*} + \left(\widehat{\boldsymbol{\eta}^*}\right)^2 \frac{(1-\cos\theta)}{\sin^2\theta} \\ &= \boldsymbol{I}_3 + \widehat{\boldsymbol{\eta}^*} + \frac{\left(\widehat{\boldsymbol{\eta}^*}\right)^2}{1+\cos\theta}, \text{ for } \theta \neq 0,\pi. \end{aligned}$$

But for $\theta$ belonging to a small neighborhood of zero, $\boldsymbol{R}_{\boldsymbol{w}\to\boldsymbol{v}}$ converges smoothly to $\boldsymbol{I}_3$ since $\boldsymbol{\eta}^*$ converges to a zero vector. Hence,

$$\boldsymbol{R}_{\boldsymbol{w}\to\boldsymbol{v}} = \boldsymbol{I}_3 + \widehat{\boldsymbol{\eta}^*} + \frac{\left(\widehat{\boldsymbol{\eta}^*}\right)^2}{1+\cos\theta}, \text{ for } \theta \neq \pi.$$

■

From a numerical perspective, Proposition 2.1 is an improvement over the original Rodrigues' formula in the following ways:

1. *Eliminated one of the two singularities (singularity at $\theta = 0$)*: This is captured in the hypothesis of Proposition 2.1 where $\boldsymbol{R}_{\boldsymbol{w}\to\boldsymbol{v}}$ is provided for all $\boldsymbol{w}$ except for $\boldsymbol{w} = -\boldsymbol{v}$.

2. *Improved computational stability for $\theta \in S^1$ bounded away from $\pi$*: The DAESR algorithm demonstrated in Subsection 4.2 utilizes a threshold $\theta_t < \pi$ to compute the attitude estimate in a computationally robust manner for conditions where $\theta \in S^1$, $|\theta| \leq \theta_t$ using Proposition 2.1.

***Euler angle representation***: Euler angle representation uses three angles to represent a unique orientation in $SO(3)$. The angle definitions depend on the chosen axis representation. Just like for the equivalent axis representation, $\boldsymbol{R}$ cannot be globally described using a single Euler angle representation. We will be using ZYX-Euler angle representation which is also referred to as yaw ($\psi$), pitch ($\delta$) and roll ($\gamma$) parameterization. There are two singularity points in this representation which occurs at $\delta = \pm\frac{\pi}{2}$. ZYX-Euler angle representation is a moving frame representation, and it rotates $\{\mathbb{F}_1\}$ to $\{\mathbb{F}_2\}$ by rotating about the $z$-axis of $\{\mathbb{F}_1\}$ by $(-\psi)$ followed by rotation about the rotated $y$-axis by $(-\delta)$ and ends with a rotation about the rotated $x$-axis by $(-\gamma)$. Therefore, $\boldsymbol{R}_{F_2}^{F_1} = \boldsymbol{R}_{\boldsymbol{e}_3}(\psi)\boldsymbol{R}_{\boldsymbol{e}_2}(\delta)\boldsymbol{R}_{\boldsymbol{e}_1}(\gamma)$ where $\boldsymbol{e}_1$ is the $x$-axis, $\boldsymbol{e}_2$ is the $y$-axis and $\boldsymbol{e}_3$ is the $z$-axis after appropriate rotations.

## 2.2 What is the minimal information needed for complete attitude estimation?

We answer this question using a recent work on decomposition of rotation matrices into Euler angles [7]. The general rotation matrix linking two vectors $\boldsymbol{v}$ and $\boldsymbol{w}$ can be captured by $\boldsymbol{v} = \boldsymbol{R}\boldsymbol{w}$, where

$$\boldsymbol{R} = \boldsymbol{R}_1\boldsymbol{R}_2 = \exp(\alpha\widehat{\boldsymbol{v}})\exp(\beta\widehat{\boldsymbol{e}}) \tag{5}$$

and $\widehat{\boldsymbol{e}}, \beta$ are provided by Proposition 2.1 and $\alpha \in S^1$. Here, $\exp(\cdot)$ denotes the matrix exponential function.

This interpretation can be geometrically visualized as decomposing any rotation matrix linking two frames as a concatenation of two rotation matrices $\boldsymbol{R}_1$ and $\boldsymbol{R}_2$. $\boldsymbol{R}_2$ ensures alignment of one of the axes of the body-fixed-frame to its corresponding axis in the inertial frame. $\boldsymbol{R}_1$ aligns the other two axes with the inertial frame by rotating about the aligned axis.

**Definition 2.1** *A vector correspondence is defined as a set of two vectors which are the resolution of a single free vector resolved in two different coordinate frames.*

Using the interpretation for $\boldsymbol{R}_2$, we use Proposition 2.1 to compute $\boldsymbol{R}_2$. For this computation, we require a vector correspondence pair $(\boldsymbol{v}, \boldsymbol{w})$ — vector information of a vector in the inertial frame and its resolution in the body-fixed-frame. Since the rotation matrix preserves norm, two constraints that inherently appears is that $\|\boldsymbol{v}\| = \|\boldsymbol{w}\| = 1$ and a third constraint on the information provided is $\|\boldsymbol{e}\| = 1$. Since the rotation matrix has three degrees-of-freedom, all the information provided by a vector correspondence $(\boldsymbol{v}, \boldsymbol{w})$ goes into estimation of the $\boldsymbol{R}_2 = \exp(\beta\widehat{\boldsymbol{e}})$. From (5), $\boldsymbol{R}_1$ is completely characterized by $\alpha$. In TRIAD algorithm (Subsection 4.1), we obtain information about $\alpha$ through another vector correspondence whereas in DAESR algorithm (Subsection 4.2), this information is obtained from rate gyros.

In short, the complete attitude determination requires three independent measurements.

## 2.3 What information do the sensors provide?

The inertial measurement unit (IMU) have now become ubiquitous in robotics and generally comprise of three sensors — accelerometers, magnetometers and gyroscopes. In this subsection, we analyze each of these sensors based on the discussion in [9]. For more detailed explanations, the reader is directed to [9][10][11].

Using an IMU that is "strapped down" to the body frame, one can measure several interesting properties associated with the body-fixed-frame $\{\mathbb{G}\}$ with respect to the inertial frame $\{\mathbb{I}\}$. We define $\{\mathbb{I}\} = \{\boldsymbol{e}_1, \boldsymbol{e}_2, \boldsymbol{e}_3\}$ where $\boldsymbol{e}_1$ is aligned along the direction towards Earth's magnetic north and $\boldsymbol{e}_3$ is aligned radially outwards from the Earth's surface. We define $\{\mathbb{G}\} = \{\boldsymbol{e}'_1, \boldsymbol{e}'_2, \boldsymbol{e}'_3\}$. Here, $\boldsymbol{e}_i$ and $\boldsymbol{e}'_i$, for $i \in \{1, 2, 3\}$, are standard basis vectors for $\{\mathbb{I}\}$ and $\{\mathbb{G}\}$ respectively.

***Accelerometers***: Let $\boldsymbol{a}_b$ denote the instantaneous linear acceleration of $\{\mathbb{G}\}$ relative to $\{\mathbb{I}\}$, expressed in $\{\mathbb{I}\}$. The accelerometer readout $\boldsymbol{a}_s$ can be modelled as:

$$\boldsymbol{a}_s = \boldsymbol{R}_I^G(\boldsymbol{a}_b - \boldsymbol{g}) + \boldsymbol{b}_a + \boldsymbol{\mu}_a$$

where $\boldsymbol{g} = -\|\boldsymbol{g}\|\boldsymbol{e}_3$ is the *acceleration due to gravity* vector expressed in $\{\mathbb{I}\}$, $\boldsymbol{b}_a$ is the accelerometer bias term and $\boldsymbol{\mu}_a$ denotes additive measurement noise. Normally, $\|\boldsymbol{g}\| \approx 9.8$ and $\|\boldsymbol{b}_a\|$ and $\|\boldsymbol{\mu}_a\|$ have much lower value compared to $\|\boldsymbol{g}\|$. Therefore, $\boldsymbol{R}_I^G\boldsymbol{g}$ dominates the value of $\boldsymbol{a}_s$ for low values of $\boldsymbol{a}_b$. This motivated the use of the normalized accelerometer readout, $\boldsymbol{a} = \frac{\boldsymbol{a}_s}{\|\boldsymbol{a}_s\|} = -\boldsymbol{R}_I^G\boldsymbol{e}_3$, as a low-frequency estimate of the unit vector corresponding to the inertial $z$-axis expressed in the body-fixed-frame [6][9].

***Magnetometers***: The magnetometers provide measurements of the magnetic field $\boldsymbol{m}_s$. The readout is modelled as:

$$\boldsymbol{m}_s = \boldsymbol{R}_I^G\boldsymbol{e}_1 + \boldsymbol{b}_m + \boldsymbol{\mu}_m$$

where $\boldsymbol{e}_1$ is the direction of the Earth's magnetic field, $\boldsymbol{b}_m$ is the body-fixed-frame expression for the local magnetic disturbance and $\boldsymbol{\mu}_m$ denotes measurement noise. Note that the inertial frame is assumed to have one of its axis $\boldsymbol{e}_1$ aligned with the direction of the Earth's magnetic north. Usually, $\|\boldsymbol{\mu}_m\|$ is quite small in comparison with $\|\boldsymbol{b}_m\|$ and $\|\boldsymbol{e}_1\| = 1$. However, the local magnetic disturbance $\boldsymbol{b}_m$ can be very significant if the robot is a ground robot or if the IMU is fixed close to the electric motors. We define $\boldsymbol{m}$ as the normalized magnetometer readout.

It is well known that Earth's magnetic north does not coincide with the true north (geographic) causing a magnetic declination to appear. The correction matrix for the declination is $\boldsymbol{R}_{\boldsymbol{e}_3}(\theta_d)$ where $\theta_d$ is the angle of magnetic declination [12] [13]. This correction is seen in the TRIAD algorithm (Subsection 4.1).

***Rate gyros***: The rate gyro measures angular velocity $\boldsymbol{\omega}_g$ of $\{\mathbb{G}\}$ relative to $\{\mathbb{I}\}$ expressed in the body-fixed-frame $\{\mathbb{G}\}$. The readout is modelled as:

$$\boldsymbol{\omega}_g = \boldsymbol{\omega} + \boldsymbol{b}_g + \boldsymbol{\mu}_g$$

where $\boldsymbol{\omega}$ denotes the true value, $\boldsymbol{\mu}_g$ denotes additive measurement noise and $\boldsymbol{b}_g$ denotes a constant (or slowly time-varying) gyro bias. By definition, $\boldsymbol{\omega} = ((\boldsymbol{R}_G^I)^\top \dot{\boldsymbol{R}}_G^I)^\vee$.

# 3 Distinction between deterministic and optimal attitude estimation

As described in [14], attitude estimation techniques can be classified into two groups — deterministic and optimal. Table 1 summarizes the difference in the approaches.

| Property | Deterministic Estimation | Optimal Estimation |
|---|---|---|
| Approach to estimation | Algebraic Constraints | Minimizing a cost function like Wahba's Problem [19] |
| General role in estimation | Initial Estimate | Improves the estimate |
| Examples | DAESR [6], TRIAD [8], DCM algorithm [17] | Nonlinear filter [9], Kalman filters [3] |
| Information Requirement | Lower | Higher |
| Immunity to Noise | Lower | Higher |
| Computational cost | Lower | Higher |
| Tuning | Absent | Present |

Table 1: Differences between deterministic and optimal estimation approaches with the favourable traits highlighted [14][18].

Deterministic attitude estimation aims to estimate the attitude by solving a set of algebraic constraints developed from the properties of the rotation matrices and sensors. They have a lower immunity to noise as they try to use minimal information to estimate the attitude. Two deterministic attitude estimation techniques, TRIAD and DAESR, are discussed in Section 4.

Optimal attitude estimation estimates the attitude by optimizing some cost function. Optimal attitude estimation using Kalman filter is an active research area [15] [16]. As expected, optimal attitude estimators have higher immunity to noise. Nonlinear complementary filter [9] is another popular optimal attitude estimator and is discussed briefly in Section 5.

# 4 Deterministic attitude estimation

We analyze two deterministic attitude estimation algorithms — TRIAD and DAESR. TRIAD algorithm is a straightforward extension of the discussion in Subsection 2.2. DAESR algorithm, on the other hand, uses the structure of the attitude estimation problem to best fuse the data from two measurement devices accelerometer and rate gyros to produce a deterministic attitude estimate. The performance of these algorithms are compared in Section 6.

Under the assumptions of low body acceleration and absence of strong magnetic fields disturbing Earth's magnetic field, these algorithms provides $R_G^I$ as defined in Subsection 2.3. These algorithms can be extended to provide the attitude estimates between coordinate frames different from $\{\mathbb{G}\}$ and $\{\mathbb{I}\}$ by appropriate rotational transformations [6].

## 4.1 TRIAD algorithm

The TRIAD algorithm utilizes two vector informations with the constraint that the vectors are mutually orthogonal [5]. As discussed in Subsection 2.2, these two vector informations are sufficient to estimate the attitude in a deterministic fashion. Conventionally, in robotics especially, these two vector informations are the readouts from an accelerometer and a magnetometer. The estimate is corrected for the magnetic declination as described in Subsection 2.3. The TRIAD algorithm is described in Algorithm 1.

**Algorithm 1** Description of TRIAD

**Input:** Normalized accelerometer ($\boldsymbol{a}$) and magnetometer ($\boldsymbol{m}$) readouts, and $\theta_d$ magnetic declination

**Output:** $\boldsymbol{R}_{\text{TRIAD}}$

**procedure** TRIAD($\boldsymbol{a}, \boldsymbol{m}, \theta_d$)
  $\boldsymbol{m}_c \leftarrow \frac{(\boldsymbol{m}-(\boldsymbol{m}.\boldsymbol{a})\boldsymbol{a})}{\|\boldsymbol{m}-(\boldsymbol{m}.\boldsymbol{a})\boldsymbol{a}\|}$ ▷ Gram-Schmidt orthogonalization to correct bias
  $\boldsymbol{R}_I^G \leftarrow \boldsymbol{R}_{\boldsymbol{e}_3}(\theta_d)\,[\boldsymbol{m}_c\ (-\boldsymbol{a} \times \boldsymbol{m}_c)\ (-\boldsymbol{a})]$ ▷ Known columns vectors
  $\boldsymbol{R}_{\text{TRIAD}} \leftarrow \left(\boldsymbol{R}_I^G\right)^\top$ ▷ Declination corrected $\boldsymbol{R}_{\text{TRIAD}}$, $\boldsymbol{R}_G^I = \left(\boldsymbol{R}_I^G\right)^\top$
  **return** $\boldsymbol{R}_{\text{TRIAD}}$
**end procedure**

## 4.2 DAESR algorithm

The work presented in [6] aims to estimate the attitude from a single vector correspondence pair and body angular velocity readings. Since the estimation approach is deterministic, the discussion in Section 3 carries forward. An important distinction between TRIAD and DAESR is that DAESR need not depend on magnetometer readings making it a suitable choice for attitude estimation of spherical robots and in environments where Earth's magnetic fields are distorted [6]. We choose a vector correspondence such that the resolution of a vector $\boldsymbol{v}(t) \in S^2$, measured in the body-fixed-frame, is a constant vector $\boldsymbol{v}_e \in S^2$ in the inertial frame. In other words, DAESR computes a time-varying attitude estimate $\boldsymbol{R}_{\text{est}} \in SO(3)$ such that $\boldsymbol{v}_e = \boldsymbol{R}_{\text{est}}\boldsymbol{v}(t)$ and $\boldsymbol{R}_{\text{est}}^\top \dot{\boldsymbol{R}}_{\text{est}} = \boldsymbol{\omega}(t)$ where $\boldsymbol{\omega}(t)$ is the rate gyro readings.

In this section, DAESR algorithm is applied to estimate the attitude $\boldsymbol{R}_{\text{est}}$ from accelerometer and rate gyro readings under low body acceleration conditions, that is, esti-

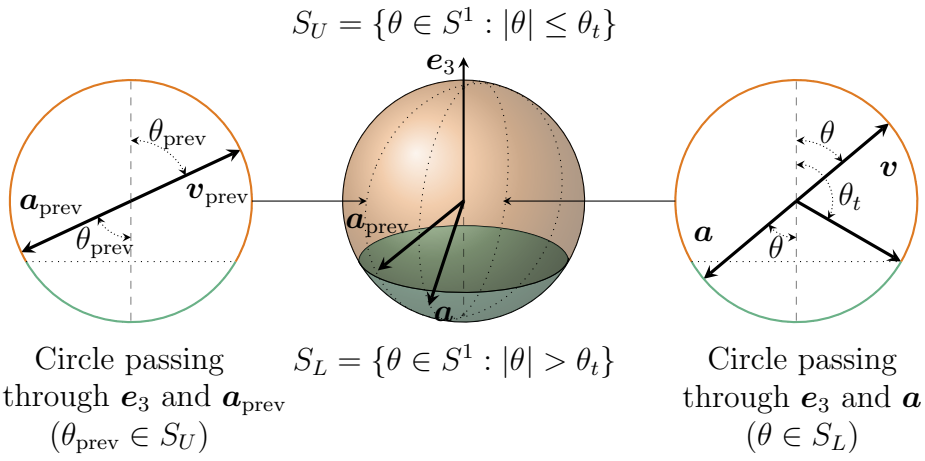


Figure 2: Definitions of $\theta$, $\theta_t$, $\theta_{\text{prev}}$, $S_U$ and $S_L$ (Based on Fig. 2 in [6])

mate $\boldsymbol{R}_{\text{est}}$ using $\boldsymbol{v}_e = \boldsymbol{e}_3$, $\boldsymbol{v}(t) = -\boldsymbol{a}(t)$ and $\boldsymbol{\omega}_g(t)$ where $\boldsymbol{a}(t)$ is the normalized accelerometer reading as defined in Subsection 2.3. Carrying forward the definitions for the frames $\{\mathbb{I}\}$ and $\{\mathbb{G}\}$ in Subsection 2.3, we use the following notation to describe DAESR:

1. Body-fixed-frame attached to the IMU is denoted as $\{\mathbb{G}\}$.

2. Inertial frame which has one of its axes along the direction of the constant vector $\boldsymbol{e}_3$ is denoted as $\{\mathbb{I}\}$. It is rotated about $\boldsymbol{e}_3$ so that $\{\mathbb{I}\}$ coincides with $\{\mathbb{G}\}$ at the start of the experiment.

3. Intermediary non-inertial frame obtained by rotating $\{\mathbb{I}\}$ by $\alpha(t) \in S^1$ about $\boldsymbol{e}_3$ is denoted as $\{\mathbb{I}_1\}$. By definition, $\boldsymbol{R}^I_{I_1} = \boldsymbol{R}_{\boldsymbol{e}_3}(\alpha(t))$ and $\alpha(0) = 0$. Hence, at the start of the experiment, $\{\mathbb{I}_1\}$, $\{\mathbb{I}\}$ and $\{\mathbb{G}\}$ coincide.

Similar to the definitions of $\{\mathbb{I}\}$ and $\{\mathbb{G}\}$, we define $\{\mathbb{I}_1\} = \{\boldsymbol{e}^*_1, \boldsymbol{e}^*_2, \boldsymbol{e}^*_3\}$ where $\boldsymbol{e}^*_i$, for $i \in \{1, 2, 3\}$, is the standard basis for $\{\mathbb{I}_1\}$. The rotational displacement between the body-fixed-frame $\{\mathbb{G}\}$ and an inertial frame $\{\mathbb{I}\}$ is given by

$$\boldsymbol{R}^I_G = \boldsymbol{R}^I_{I_1}\boldsymbol{R}^{I_1}_G = \boldsymbol{R}_{\boldsymbol{e}_3}(\alpha(t))\boldsymbol{R}_{\boldsymbol{v}(t)\to\boldsymbol{v}_e}. \tag{6}$$

**Remark 4.1** *For this subsection, we drop the explicit reference to the time-dependence of the variables for brevity. We also assume low noise in the rate gyro, i.e,* $\boldsymbol{\omega}_g \approx \boldsymbol{\omega}$.

DAESR uses two approaches to estimate the attitude — Euler-angle approach and equivalent axis approach [6]. While $\boldsymbol{R}_{\text{est}} = \boldsymbol{R}_{\boldsymbol{e}_3}(\alpha)\boldsymbol{R}_C\boldsymbol{R}_V$, the differences in these approaches is in the methodology used to compute $\alpha$ and $\boldsymbol{R}_V$. These differences are tabulated in Table 2 and the DAESR algorithm is summarized in Algorithm 2. Figure 2 defines the variables used in DAESR.

We define $\theta$ to be the angle between the vectors $\boldsymbol{v} = -\boldsymbol{a}$ and $\boldsymbol{v}_e = \boldsymbol{e}_3$ and $\theta_{\text{prev}}$ to be the angle in the last measurement. The approach used to estimate $\boldsymbol{R}_{\text{est}}$ is decided by the value of $\theta$. The definitions of $S_L$ and $S_U$ ensure that the singularity points of each of the approaches, listed in Table 2, are avoided when computing $\boldsymbol{R}_V$. The equivalent axis approach was discussed in Subsection 2.1. When using the Euler-angle approach, we define $\boldsymbol{R}_E = \boldsymbol{R}_{\boldsymbol{e}_2}(\delta)R_{\boldsymbol{e}_1}(\gamma)$ where $(\psi, \delta, \gamma)$ is the ZYX-Euler angle representation of $\boldsymbol{R}_{\boldsymbol{v}\to\boldsymbol{v}_e}$ and absorb the yaw $\psi$ into the definition of $\alpha$ [6]. By definition, $\boldsymbol{R}^\top_{\boldsymbol{v}\to\boldsymbol{v}_e}\boldsymbol{R}_E = \boldsymbol{R}_{\boldsymbol{e}_3}(\psi)$. We compute $\boldsymbol{R}_E$ using the following proposition:

**Proposition 4.1** *Given $\theta \in S_L$ and the normalized accelerometer readings $\boldsymbol{a} = (a_x, a_y, a_z)$,*

$$\boldsymbol{R}_E = \begin{bmatrix} \sqrt{a_y^2 + a_z^2} & -\frac{a_x a_y}{\sqrt{a_y^2+a_z^2}} & -\frac{a_x a_z}{\sqrt{a_y^2+a_z^2}} \\ 0 & -\frac{a_z}{\sqrt{a_y^2+a_z^2}} & \frac{a_y}{\sqrt{a_y^2+a_z^2}} \\ -a_x & -a_y & -a_z \end{bmatrix}.$$

The rotation angle about $\boldsymbol{e}_3$, $\alpha$, is determined by integration of $\boldsymbol{e}_3^\top \Omega$ and the value of $\alpha$ depends where $\theta$ and $\theta_{\text{prev}}$ lie. Estimation of $\boldsymbol{e}_3^\top \Omega$ requires the knowledge of $\boldsymbol{a}$, $\dot{\boldsymbol{a}}$ and $\theta$. We estimate $\dot{\boldsymbol{a}}$ by the relation $\dot{\boldsymbol{a}} = \boldsymbol{\omega} \times \boldsymbol{a}$ from Shuster's work [2]. We set $\alpha$ as zero when $\theta_{\text{prev}}$ is not in the set containing $\theta$ and update $\boldsymbol{R}_C$ by approximating that both $\boldsymbol{R}_L$ and $\boldsymbol{R}_U$ can be estimated accurately in the neighborhood of $\theta_t = \frac{2\pi}{3}$.

The reader is directed to [6] for a more rigorous discussion of DAESR algorithm. The development of DAESR is not restricted to using $\boldsymbol{v} = -\boldsymbol{a}$ and is generalizable to any vector correspondence pair. The MATLAB implementation of this algorithm for $\boldsymbol{v} = -\boldsymbol{a}$ is available at: `https://bitbucket.org/abyvinod/daesr.git`.

# 5 Optimal attitude estimation— Passive nonlinear complimentary filter without bias correction

We now discuss a popular optimal attitude estimator — passive nonlinear complimentary filter without bias correction from [9]. This filter uses a measured estimate of the attitude to give a robust estimate of the attitude based on the tuned optimal algorithm gain $k_P$. Since the estimator uses a complimentary filter approach, by varying $k_P$, one can vary the trust on the gyroscope readouts and the predicted angular velocities to construct the estimated rotation matrix by integration.

From [9, Equation 10], we have:

$$\dot{\boldsymbol{R}}_{\text{est}} = \boldsymbol{R}_{\text{est}}(\widehat{\boldsymbol{\omega}}_g(t) + k_P \widehat{\boldsymbol{\omega}}_f(t))$$

with the rate gyro readouts $\widehat{\boldsymbol{\omega}}_g(t) \in \mathfrak{so}(3)$, the predicted velocity term $\widehat{\boldsymbol{\omega}}_f(t) = \frac{\boldsymbol{R}_{\text{est}}^\top \boldsymbol{R}_y - \boldsymbol{R}_y^\top \boldsymbol{R}_{\text{est}}}{2} \in \mathfrak{so}(3)$ and the measured estimate of the attitude $\boldsymbol{R}_y$. Therefore, from the zero-order sampling approximation for a sampling period of $\Delta T$, the attitude estimate $\boldsymbol{R}_{\text{est}}$ is described by the following equation:

$$\boldsymbol{R}_{\text{est}}[n+1] = \boldsymbol{R}_{\text{est}}[n] \exp\left((\widehat{\boldsymbol{\omega}}_g[n] + k_P \widehat{\boldsymbol{\omega}}_f[n])\Delta T\right)$$

where exp() is the matrix exponential function which provides the rotation matrix corresponding to a rotation of $\|\boldsymbol{\omega}_g(t) + k_P \boldsymbol{\omega}_f(t)\|\Delta T$ along the screw $(\boldsymbol{\omega}_g(t) + k_P \boldsymbol{\omega}_f(t))$. The robustness analysis of this nonlinear estimator was shown using Lyapunov stability theory [9].

# 6 Performance of the estimation algorithms

In this section, we reproduce the process of validation of the DAESR algorithm as presented in [6]. We use the spherical robot developed at the Dynamics and Control Lab, IIT Madras (Figure 3) as the test-bed for comparing the attitude estimation algorithms

| Property | Equivalent axis method ($\boldsymbol{R}_U$) | Euler-angle method ($\boldsymbol{R}_L$) |
|---|---|---|
| $\boldsymbol{R}_U$ and $\boldsymbol{R}_L$ | $\boldsymbol{R}_{\boldsymbol{e}_3}(\alpha)\boldsymbol{R}_C\boldsymbol{R}_V$ | |
| $\alpha$ | $\begin{cases} \alpha + (\boldsymbol{e}_3^\top \Omega)\Delta T & \theta_{\text{prev}} \in S_x \\ 0 & \theta_{\text{prev}} \notin S_x \end{cases}$ | for $\theta \in S_x$, $S_x \in \{S_L, S_U\}$ |
| $\boldsymbol{e}_3^\top \Omega$ | $\frac{a_x\dot{a}_y - a_y\dot{a}_x}{1-a_z}$ | $\frac{a_x(a_y\dot{a}_z - a_z\dot{a}_y)}{1-a_x^2}$ |
| Correction matrix $\boldsymbol{R}_C$ | $\boldsymbol{R}_C = \boldsymbol{R}_L\boldsymbol{R}_{\boldsymbol{v}\to\boldsymbol{v}_e}^\top$ only when $\theta_{\text{prev}} \in S_L$ | $\boldsymbol{R}_C = \boldsymbol{R}_U\boldsymbol{R}_E^\top$ only when $\theta_{\text{prev}} \in S_U$ |
| $\boldsymbol{R}_V$ | $\boldsymbol{R}_{\boldsymbol{v}\to\boldsymbol{v}_e}$ using (3) | $\boldsymbol{R}_E$ using Proposition 4.1 |
| Singularity points | $\theta = \pi$ | $\theta = \pm\frac{\pi}{2}$ |
| Region of validity | $\theta \in S_U \triangleq \{\phi \in S^1 : \phi \in [-\frac{2\pi}{3}, \frac{2\pi}{3}]\}$ | $\theta \in S_L \triangleq S^1 \setminus S_L$ |

Table 2: Table describing various components in the DAESR algorithm. $\cos\theta = \boldsymbol{a}^\top\boldsymbol{e}_3$, $\cos\theta_{\text{prev}} = \boldsymbol{a}_{\text{prev}}^\top\boldsymbol{e}_3$, $\dot{\boldsymbol{a}} = \boldsymbol{\omega} \times \boldsymbol{a}$, $\Delta T$ is the sampling period for the sensors. Note that the regions of validity avoids the singularity points.

**Algorithm 2** DAESR algorithm (Detailed algorithm can be found in [6] and expressions for $\boldsymbol{R}_L, \boldsymbol{R}_U$ are provided in Table 2)

**Input:** Current and last accelerometer readings $(\boldsymbol{a}, \boldsymbol{a}_{\text{prev}})$ and current rate gyro $(\boldsymbol{\omega})$ readings, $\boldsymbol{R}_C = \boldsymbol{I}_3$ and $\alpha = 0$. $\boldsymbol{R}_C, \alpha$ are constantly fed back.

**Output:** $[\boldsymbol{R}_{\text{est}}, \boldsymbol{R}_C, \alpha]$

**procedure** DAESR($\boldsymbol{a}, \boldsymbol{a}_{\text{prev}}, \boldsymbol{\omega}, \boldsymbol{R}_C, \alpha$)
  $\cos\theta \leftarrow ba^\top\boldsymbol{e}_3$
  $\cos\theta_{\text{prev}} \leftarrow \boldsymbol{a}_{\text{prev}}^\top\boldsymbol{e}_3$
  **if** $\theta \in S_U$ **then**
    **if** $\theta_{\text{prev}} \in S_L$ **then**
      $\boldsymbol{R}_{\text{est}} \leftarrow \boldsymbol{R}_L$; *Update* $\boldsymbol{R}_C$ *and set* $\alpha = 0$
    **else**
      $\boldsymbol{R}_{\text{est}} \leftarrow \boldsymbol{R}_U$; *Update* $\alpha$
    **end if**
  **else** ▷ $\theta \in S_L$
    **if** $\theta_{\text{prev}} \in S_U$ **then**
      $\boldsymbol{R}_{\text{est}} \leftarrow \boldsymbol{R}_U$; *Update* $\boldsymbol{R}_C$ *and set* $\alpha = 0$
    **else**
      $\boldsymbol{R}_{\text{est}} \leftarrow \boldsymbol{R}_L$; *Update* $\alpha$
    **end if**
  **end if**
  **return** $[\boldsymbol{R}_{\text{est}}, \boldsymbol{R}_C, \alpha]$
**end procedure**

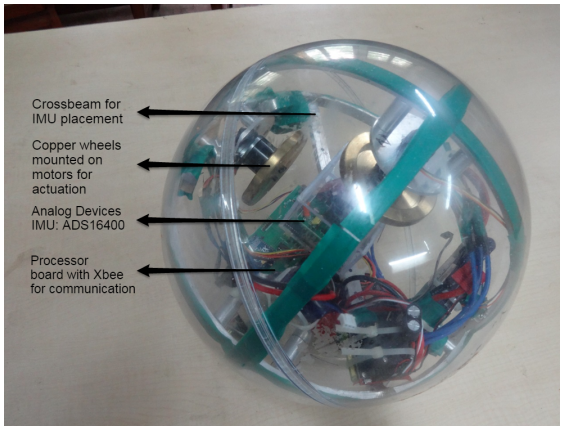


Figure 3: Experimental setup - spherical robot

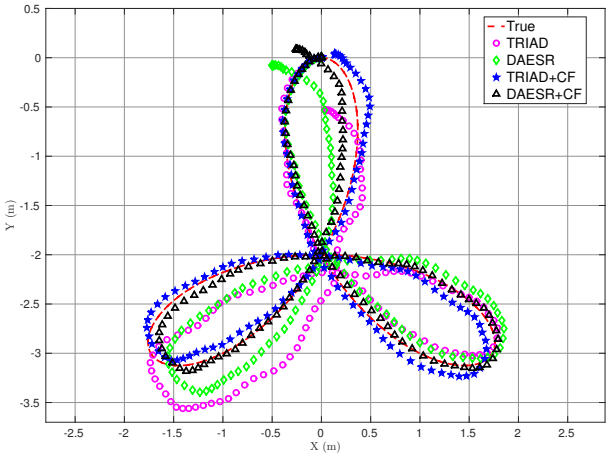


Figure 4: Spherical robot on trifolium path (The estimated positions are rotated to avoid the possible mismatch in initial orientation)

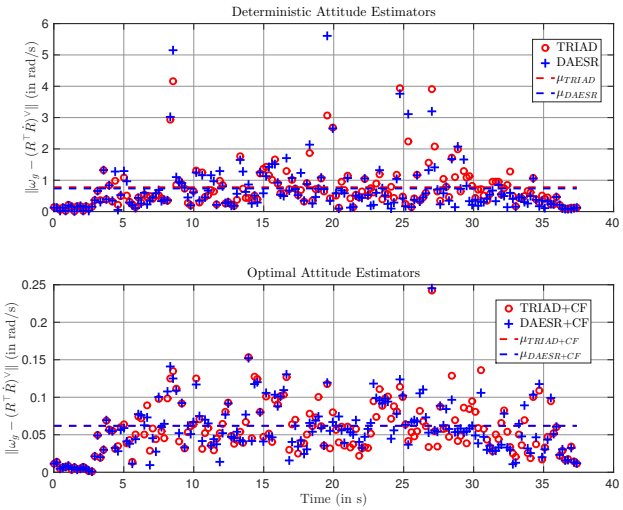


Figure 5: Magnitude of error between measured and estimated body angular velocities when the spherical robot is on a trifolium path

discussed in this chapter. A spherical robot has five degrees-of freedom — two translational $(x, y)$ and three rotational ($\boldsymbol{R}$). The inertial measurement unit used is Analog Devices ADIS16400 and is placed at the center of the bot.

For brevity, we analyze the case when the spherical robot is rolled on a *trifolium* path. The DAESR attitude estimate is compared with the TRIAD algorithm as a standalone algorithm and as inputs to the passive nonlinear complementary filter proposed in [9], denoted by DAESR+CF and TRIAD+CF respectively. The passive nonlinear complementary filter is implemented without bias correction and the optimal algorithm gain $k_P$ was chosen as 0.05 by tuning for TRIAD as the measured estimate of attitude.

The position of the spherical robot can be computed from the non-holonomic constraints derived from the spherical robot dynamics,

$$\dot{x} = r\boldsymbol{e}_2^\top \boldsymbol{R}\boldsymbol{\omega},$$
$$\dot{y} = -r\boldsymbol{e}_1^\top \boldsymbol{R}\boldsymbol{\omega}$$

with $r$ as the radius of the spherical robot. Figure 4 shows the robustness of the attitude estimates to a first-order integration. Figure 5 shows the magnitude of the difference in the estimated body angular velocity and the measured angular velocity. As expected, the optimal attitude estimations, TRIAD+CF and DAESR+CF, have much lower error as compared to the deterministic attitude estimation, TRIAD and DAESR. Among the deterministic attitude estimators, it is found that DAESR algorithm performs better than TRIAD as a standalone estimator and as a measured estimate for the complimentary filter. Further analysis of the performance of these algorithms can be found in [6]. A video of the experimental validation of DAESR is available at `http://youtu.be/ounyQH\_W2os`.

# 7 Concluding Remarks

In this chapter, we looked at two attitude estimation approaches — deterministic and optimal. We pointed out the differences in these approaches. We also analyzed the sensors commonly used in attitude estimation and discussed the minimal information required for complete attitude estimation. In the deterministic estimation approaches, two algorithms were discussed — TRIAD and DAESR. In the optimal estimation approach, the passive nonlinear complimentary filter without bias correction was discussed.

# References


[1] R. N. Murray, Z. Li, and S. Sastry, *A Mathematical Introduction to Robotics Manipulation*, 1st ed. CRC Press, 1994.

[2] M. Shuster, "A Survey of Attitude Representations", *The Journal of the Astronautical Sciences*, 41(4), pp. 439-517, 1981.

[3] N. Madinehi, "Rigid body attitude estimation: An overview and comparative study", *University of Western Ontario - Electronic Thesis and Dissertation Repository*, Paper 1259, 2013.

[4] T. Lee, M. Leoky and N. H. McClamroch, "Geometric tracking control of a quadrotor UAV on SE (3)", *IEEE Conf. on Decision and Control*, 49, pp. 5420-5425, 2010.

[5] H. D. Black, "A passive system for determining the attitude of a satellite", *AIAA Journal*, 2(7), pp. 1350-1351, 1964.

[6] A. P. Vinod, A. D. Mahindrakar, S. Bandyopadhyay and V. M. Muralidharan, "A Deterministic Attitude Estimation Using a Single Vector Information and Rate Gyros", *IEEE Trans. Mechatronics*, 20(5), pp. 2630-2636, 2015.

[7] G. Piovan and F. Bullo, "On Coordinte-Free Rotation Decomposition: Euler angles about Arbitrary Axes", *IEEE Trans. Robotics*, 28(3), pp. 728-733, 2012.

[8] M. D. Shuster and S. D. Oh, "Three-Axis Attitude Determination from Vector Observations", *Journal of Guidance and Control*, 4 (1), pp. 70-77, 1981.

[9] R. Mahony, T. Hamel and J. M. Pflimlin, "Nonlinear Complementary Filters on the Special Orthogonal Group", *IEEE Trans. Automatic Control*, 53 (5), pp. 1203-1218, 2008.

[10] M. Grewal and A. Andrews, "How Good Is Your Gyro [Ask the Experts]", *IEEE Control Systems Magazine*, 30(1), pp. 12-86, 2010.

[11] J. J. Allen, *Micro Electro Mechanical System Design*, CRC Press, 2005.

[12] V. Renaudin, M. H. Afzal and G. Lachapelle, "Complete triaxis magnetometer calibration in the magnetic domain", *Journal of Sensors*, 2010, Article ID 967245, 10 pages, 2010.

[13] Magnetic-Declination.com, "Find the magnetic declination at your location", Accessed April 27, 2016. `www.magnetic-declination.com`.

[14] J. R. Wertz, *Spacecraft Attitude Determination and Control*, Kluwer Academic Publishers, Dordrecht, 1978.

[15] J. L. Crassidis, F. L. Markley and Y. Cheng, "Survey of nonlinear attitude estimation methods", *Journal of Guidance, Control, and Dynamics* 30(1) pp. 12-28, 2007.

[16] J. L. Crassidis and J. L. Junkins, *Optimal estimation of dynamic systems*, CRC press, 2011.

[17] W. Premerlani and P. Bizard, "Direction Cosine Matrix IMU: Theory", 2009. [Online]. Accessed April 27, 2016. Available: `gentlenav.googlecode.com/files/DCMDraft2.pdf`

[18] M. Shuster, "Deterministic Three-Axis Attitude Determination", *The Journal of the Astronautical Sciences*, 52(3), pp. 405-419, 2004.

[19] G. Wahba, "A least squares estimate of satellite attitude", *SIAM review* 7(3), pp. 409-409, 1965.